



THE AA GRAPHITE DEPOSIT, BELLA COOLA AREA, BRITISH COLUMBIA: EXPLORATION IMPLICATIONS FOR THE COAST PLUTONIC COMPLEX (92M/15)

By Nathalie Marchildon, George J. Simandl and Kirk D. Hancock

KEYWORDS: Industrial minerals, graphite, crystalline flake, granulite facies, Coast Plutonic Complex, thermobarometry, retrograde metamorphism, exploration.

INTRODUCTION

Natural graphite is a well known high unit-value industrial mineral with a wide range of applications (Taylor, 1992; Simandl, 1992; Simandl *et al.*, 1992). The major uses are shown in Figure 3-3-1. Commercial graphite concentrates are classified into four major categories: crystalline lumps, crystalline flakes, powder and "amorphous" powder. Crystalline flake graphite is hosted by amphibolite to granulite grade metasedimentary rocks. The term "lump and chip" graphite refers to high-grade vein-type ore fragments typically 0.5 to 0.8 centimetre in size. Crystalline powder is produced as the result of excessive milling of flake graphite. Microcrystalline graphite, commonly called "amorphous" graphite, is produced from metamorphosed coal seams.

The most important technical parameters governing the price of graphite flake concentrate are graphitic carbon content, flake size, degree of crystallinity and the types of impurities. Prices of typical graphite concentrates are illustrated in Table 3-3-1. The long and medium-term outlooks for graphite consumption are positive. In the short term,

TABLE 3-3-1
TYPES OF GRAPHITE CONCENTRATES AND COSTS
PER TON (US DOLLARS)

	Grade	Price
Crystalline lumps	92/95 %C	750-1500
Crystalline large flakes	85/90 %C	650-1200
Crystalline medium flakes	85/90 %C	450-1000
Crystalline small flakes	80/95 %C	400-600
Powder (200 mesh)	80/85 %C	325-360
	90/92 %C	520-600
	95/97 %C	770-1000
	97/99 %C	1000-1300
Amorphous powder	80/85 %C	220-440

CIF UK port

(Source: *Industrial Minerals*, 1992, Number 301, page 68.)

there is an oversupply, as with most other industrial minerals, due to reduced manufacturing activity worldwide (Harries-Rees, 1992). Prices of natural graphite are expected to recover faster than most other industrial minerals as many industries have kept inventories low during the recession (Hand, 1992) and if, as forecast, China reduces graphite exports to satisfy increasing internal needs (Holroyd and McCracken, 1992). In industrialized countries the areas of fastest growth for natural graphite use are likely to be the automotive and nuclear industries (Kanan, 1992).

This study focuses on a crystalline flake graphite deposit located in southwestern British Columbia. This case study, combined with published regional data, indicates that there is excellent geological potential for world-class crystalline flake graphite deposits within the Coast Plutonic Complex. This paper discusses geological and exploration considerations and the technical aspects of metamorphism and geothermobarometry will be addressed elsewhere. Specific economic considerations, such as to mine, grade continuity and average grade for this deposit are beyond the scope of this paper.

LOCATION AND ACCESS

The AA graphite deposit is located in the Bella Coola area, approximately 500 kilometres north-northwest of Vancouver. The property is approximately 2 kilometres north of the head of South Bentinck Arm, on its western shore (Figure 3-3-2).

The fastest access to the deposit is by floatplane from the town of Port Hardy, at the northern tip of Vancouver Island, approximately 200 kilometres to the south. Alternatively, the deposit can be reached by driving to Bella Coola, 45 kilometres north of the deposit, and by floatplane from there.

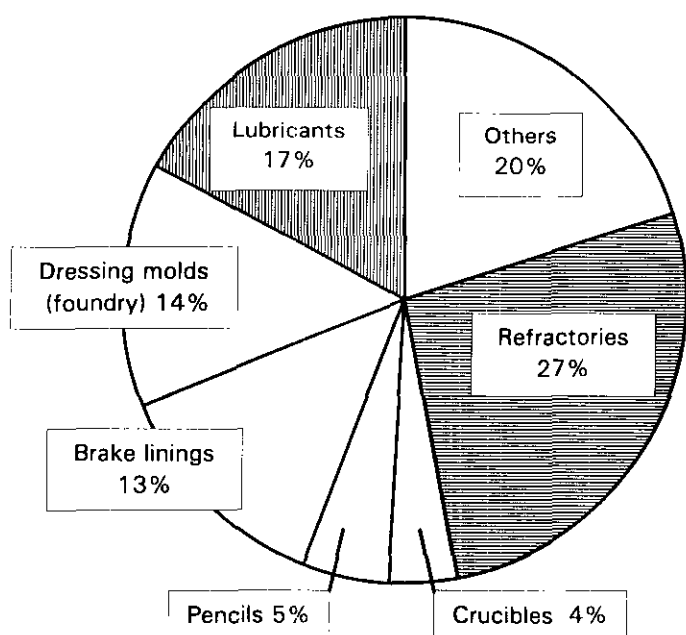


Figure 3-3-1. Natural graphite applications in the United States (from Taylor, 1992).

METHODS

Fieldwork was completed over 12 days in early July, 1992. A series of ten, 400 to 750-metre traverses, spaced 200 metres apart, were made perpendicular to the regional structural grain (northwest) on a grid centred on the graphite deposit, and more than 130 outcrops were described.

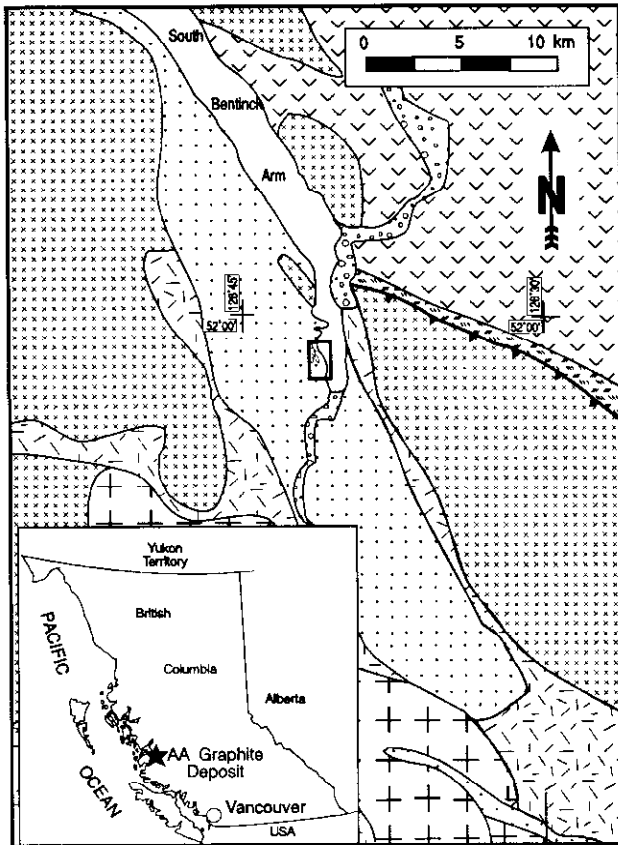
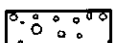
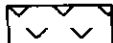
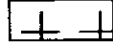
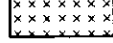
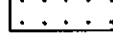
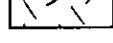



Figure 3-3-2. Regional geology of the South Bentinck Arm area, B.C. Heavy box shows area covered by Figure 3-3-3; inset shows geographical position of map area. Modified from Baer (1973) and Roddick (in preparation).

Legend

-  Quaternary alluvial and glacial deposits
-  Lower Cretaceous volcanic rocks
-  Dioritic complex
-  Undifferentiated plutonic rocks
-  Metasediments
-  Granitoid gneiss
-  Thrust fault zone

Trenches in high-grade graphitic rock were sampled and mapped in detail (1:100).

More than 50 thin sections of graphitic rocks and graphite-free country rocks and 20 thin sections of rocks from the deposit were described. Of these, six garnet-bearing rocks were analyzed using a JEOL Superprobe 733 electron microprobe to determine mineral compositions used in thermobarometric calculations. Back-scattered electron micrographs of graphite-bearing rocks were also obtained. Chemical analyses for major, minor and selected trace elements and for graphitic carbon were obtained for 13 samples from the deposit (Table 3-3-2).

REGIONAL GEOLOGY

The geological setting of the AA graphite deposit, based on 1:250 000 compilations of Baer (1973) and Roddick (in preparation), is described below and summarized in Figure 3-3-2. The volumetrically dominant rocks in the area are intrusions of the Coast Plutonic Complex (Early Cretaceous to Eocene; Baer, 1973). These rocks vary in composition from tonalite to diorite, and their precise ages are unknown. The plutons are surrounded by granitoid gneisses. The AA graphite deposit is located in a north-northeast-trending belt of metasediments running through the middle of the area covered by Figure 3-3-2. The northeast part of the area is underlain by Lower Cretaceous volcanic rocks. They are separated from intrusive rocks to the south by a regional thrust fault.

The granitoid gneisses are probably related to the intrusion of the plutons which they surround. They may represent strongly deformed intrusive material at the margins of plutons or they may have resulted from partial melting and deformation of the country rock. The metasedimentary sequences represent country rock to the intrusive complexes.

DEPOSIT GEOLOGY

The geology of the area surrounding the AA deposit is shown in Figure 3-3-3. The northern part of the map is dominated by moderately to strongly deformed granodioritic rocks. The southern part of the area is underlain by biotite-amphibole schists of metasedimentary origin. Locally, decametre to metre-scale mafic to ultramafic lenses, characterized by centimetre-scale concentrations of leucosomatic rims and crosscutting veins, may represent boudinaged mafic dikes intruding the schists and granodioritic rocks. Graphite-rich rocks outcrop in the central part of the map area, specifically in the crests of folds.

The dominant structural grain in the area is a subvertical north-northwest-trending foliation with decametre-scale folds (Figure 3-3-3). The dominant foliation trend is summarized in Figure 3-3-4. Late-kinematic folding synchronous with the development of retrograde chlorite has resulted in crenulation of this north-northwest foliation. Fold axes and resulting intersecting lineations are typically subvertical. Shear zones in the area are generally aligned with the regional foliation. Except for one extending over at least 700 metres (Figure 3-3-3), they can not be traced over any significant distance.

TABLE 3-3-2
CHEMICAL ANALYSES OF GRAPHITE-RICH ROCKS; AA GRAPHITE DEPOSIT, BRITISH COLUMBIA.

	G2/1-15	G10/2-86	G2/1-15DUP	G10/4-89	G10/1-84	G1/5-10	G2/1-16	G2/2-17	G6/2-48	G6/3-49	G10/2-85	G11, 1-94	G2/2-17/DUP
SiO ₂	66.34	64.41	66.66	66.00	62.59	65.14	59.49	62.95	47.61	58.67	64.42	70.34	64.63
Al ₂ O ₃	4.91	13.93	4.86	9.83	4.88	10.66	5.61	9.79	20.24	17.19	16.41	10.67	9.20
CaO	1.06	3.93	1.06	7.21	0.99	2.33	1.60	4.64	5.91	2.67	5.06	2.83	4.77
Cr ₂ O ₃	<0.01	<0.01	<0.01	<0.01	<0.01	<0.01	<0.01	<0.01	<0.01	<0.01	<0.01	<0.01	<0.01
Fe ₂ O ₃	4.06	3.87	4.02	3.76	2.23	3.46	2.78	2.06	9.24	6.99	3.14	1.33	2.14
K ₂ O	1.25	2.67	1.27	1.50	1.25	2.58	1.10	2.05	2.20	1.84	2.69	0.95	1.38
MgO	1.06	2.20	1.05	2.38	1.18	1.89	1.17	2.34	4.37	4.56	2.23	0.71	2.41
MnO	0.02	0.08	0.02	0.02	0.02	0.04	0.02	0.06	0.15	0.10	0.09	0.01	0.06
Na ₂ O	0.95	1.62	0.95	0.67	0.86	1.60	0.83	0.70	4.76	5.43	2.00	2.78	0.76
P ₂ O ₅	0.09	0.16	0.08	0.12	0.19	0.47	0.26	0.24	0.56	0.14	0.19	0.11	0.25
TiO ₂	0.37	0.42	0.37	0.41	0.30	0.57	0.21	0.41	1.07	0.43	0.41	0.12	0.41
LOI	19.60	6.02	19.49	9.65	24.51	9.35	26.83	13.46	2.32	1.24	3.13	10.59	13.61
C(gr)*	16.20	3.16	16.50	6.41	23.10	6.34	23.90	8.77	0.06	0.05	1.17	9.33	8.35
Ag **	0.2	<0.2	<0.2	<0.2	<0.2	<0.2	<0.2	<0.2	<0.2	<0.2	<0.2	<0.2	<0.2
Bi **	<5	<5	<5	<5	<5	<5	<5	<5	<5	<5	<5	5	<5
Cd **	2	7	1	<1	<1	6	<1	22	<1	<1	<1	1	21
Co **	189	57	191	61	35	36	45	79	67	53	32	54	78
Cr **	244	30	249	50	207	166	190	108	5	124	17	37	107
Cu **	342	114	338	84	11	136	349	124	118	188	55	37	129
Mo **	<1	12	<1	24	67	35	<1	37	<1	<1	8	24	37
Ni **	253	38	263	82	25	73	120	104	1	27	16	11	104
Pb **	44	54	40	56	38	74	54	78	134	194	240	206	42
Sr **	172	317	175	238	94	163	175	154	636	176	381	211	157
V **	287	469	296	925	1500	1827	300	1300	212	129	144	39	1320
Zn **	453	786	421	503	210	654	238	1681	133	121	239	106	1647

* graphitic carbon

** minor elements in ppm

GRANODIORITIC ROCKS

Granodioritic rocks in the area are generally coarser grained than the schists (2-5 mm grain size). The regional foliation, defined by a coarse layering of thin (<2 mm) biotite and/or amphibole-rich bands and thicker (>3 mm) quartzofeldspathic bands, is not as well expressed in these rocks as it is in the finer grained schists. The intensity of the foliation tends to decrease westwards within the granodiorite; to the northwest, the granodioritic body is essentially undeformed. In outcrop, weathered surfaces are typically yellowish white; fresh surfaces are pale to medium grey. The granodioritic rocks are more leucocratic than the schists although their mineralogy is similar except that clinopyroxene is found only in mafic and ultramafic lenses included in the granodiorite.

BIOTITE SCHISTS

Schists are usually fine to medium grained (0.5-2 mm) and display a penetrative schistosity, consistent with the regional trend and defined by the alignment of biotite and amphibole grains. These rocks weather pale grey to yellowish or brownish white. Fresh surfaces are medium to dark grey. They may display porphyroblastic textures; garnet and amphiboles are common porphyroblastic minerals. They are divided into two groups, garnet-bearing and garnet-free biotite-amphibole schists (Figure 3-3-3). Systematic trends in the distribution of these garnet-free and garnet-bearing schists suggest that the presence or absence of garnet is constrained by the bulk chemistry of the rock (aluminum content) rather than by variation in metamorphic conditions. The graphite deposit is hosted by the schists. Biotite,

hornblende, plagioclase, quartz, tremolite, actinolite, cummingtonite and clinopyroxene are the common constituent minerals of both garnet-bearing and garnet-free schists, although they may not all be present in the same rock. Sillimanite has been found in several outcrops in the southeastern part of the map area. Epidote (generally zoisite, rarely pistacite), chlorite, titanite and white mica are locally observed as minor constituents. Graphite, ilmenite, pyrite, chalcopyrite and sphalerite are the common opaque minerals and pyrrhotite has been observed as an included phase. Common accessory minerals are zircon, allanite and apatite.

Quartz and plagioclase are present in variable concentrations in all of the thin sections of schists examined. Plagioclase is locally replaced by fine-grained epidote and white mica. Biotite constitutes up to 20 volume per cent of the biotite schists. The orientation of biotite flakes generally defines the main foliation. In several instances, a late generation of biotite is developed along a later foliation. Bright red-brown biotite commonly forms less than 10 per cent of the volume in graphite-rich rocks where it is intergrown with graphite flakes (Plate 3-3-1). Green or greenish brown biotite occurs predominantly in the southern part of the mapped area. Garnet is present only locally. It generally comprises less than 5 volume per cent of the rock. It occurs in biotite-amphibole schists as strongly xenoblastic porphyroblasts (1-5 mm; in rare examples, up to 1 cm in diameter) commonly overgrown by biotite aligned with the regional schistosity. Late tectonic to post-tectonic chlorite and, less commonly, zoisite are also found as overgrowths on garnet porphyroblasts. In the southern part of the map area, it constitutes large, pre-tectonic porphyroblasts in aluminous, sillimanite-bearing schists. In all instances

garnet is pre-tectonic to early tectonic with respect to the main, regional foliation expressed in the rock. Several garnet-bearing rocks have been used to constrain metamorphic temperatures; the results are discussed below. Clinopyroxene is occasionally found as poikiloblastic relict crystals in amphibole-bearing schists. It is replaced by tremolite or hornblende. Also, it is associated with high-grade graphite concentrations where it is replaced by tremolite (Plate 3-3-2). Cummingtonite occurs as medium-sized (<2 mm) relict crystals representing less than 5 volume per cent of the schists. It is typically overgrown and replaced by tremolite (\pm actinolite) and, less commonly, by hornblende.

At least some of the cummingtonite and hornblende is present as prograde metamorphic phases. Cummingtonite has also been identified in several thin sections from

graphite-rich zones. Typically, euhedral hornblende (2–5 mm) comprises up to 15 volume per cent of the schists and colours vary from pale green to pale brown to dark brown-green. Together with biotite flakes, they define the principal foliation in the rock. The most common brownish green variety is optically zoned and often has a narrow actinolite rim (especially in strongly strained rocks). Less commonly, it is overgrown by biotite or tremolite. Locally it replaces clinopyroxene and is interpreted to be retrograde. Tremolite is fine to medium grained, generally acicular and overgrows cummingtonite, hornblende and clinopyroxene. It is interpreted as a retrograde phase.

Sillimanite represents trace to 5 volume per cent of the rock and occurs as fine prisms (2–3 mm in length and less than 500 μ m in width) aligned with the main foliation in biotite schists from the southern part of the area (Figure 3-3-3). Epidote is occasionally found in minor amounts overgrowing biotite, garnet or plagioclase. In several instances it forms fine-grained strings after biotite and is aligned with a late(?) foliation indicating syntectonic development. It was also observed in intergrowths with graphite in thin sections from graphite-rich rocks. Chlorite is pervasive as a minor retrograde phase after biotite or, less typically, after garnet. In one outcrop at the eastern margin of the map area, chlorite flakes are developed along a late cleavage which cuts and crenulates the regional foliation and is associated with outcrop-scale folds. This indicates

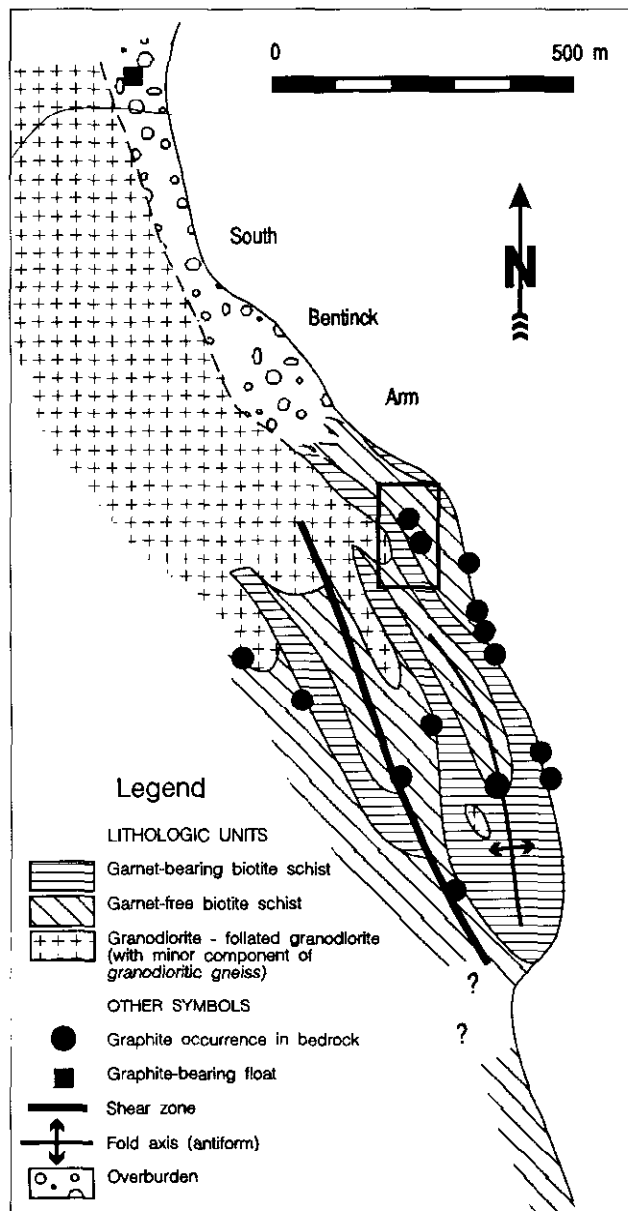


Figure 3-3-3. Local geology of the AA graphite deposit. Box is position of detailed map in Figure 3-3-5.

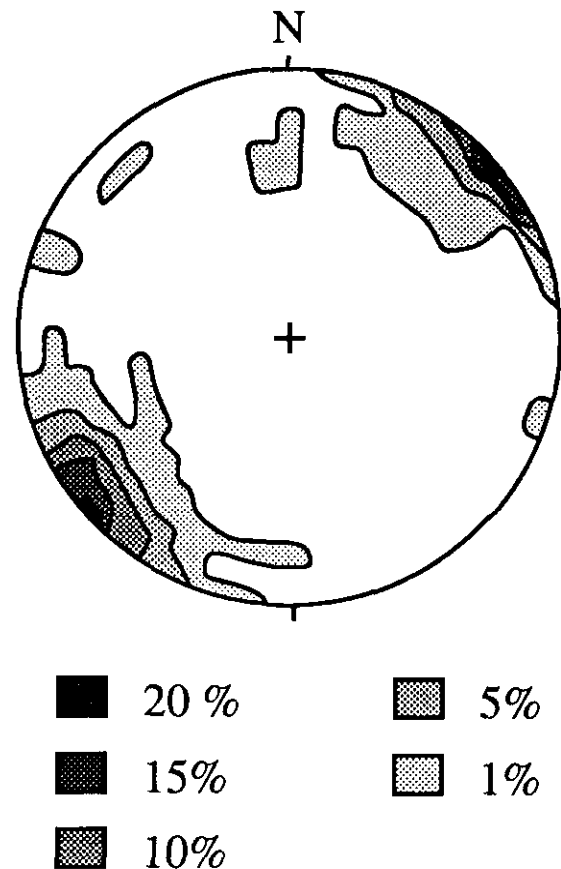


Figure 3-3-4. Stereonet projection of poles to main foliation in the area of the AA graphite deposit. n = 68.

that deformation was continuing during retrograde metamorphic recrystallization in rocks of the area. Chlorite is extensively developed in thin, post-tectonic veinlets.

Titanite is a relatively abundant (2–3 volume %) late phase in graphite-poor and graphite-free rocks where it is concordant with the regional foliation and developed at edges of hornblende and biotite grains. Traces of zircon are pervasive in the schists. It occurs in two varieties which often coexist in the same thin section. The first variety consists of large (200–500 μm), sometimes zoned, rounded to euhedral grains that are erratically distributed in the matrix. These are interpreted to be premetamorphic zircons. The second variety of zircon forms clots of very small (<100 μm) euhedral grains commonly found at the interface between biotite grains and other matrix minerals. The latter variety may overgrow euhedral zircon grains and is interpreted to be synmetamorphic.

Pyrite is found in two texturally distinct generations, commonly in rocks containing graphite. An early pyrite is present in trace concentrations, as fine-grained, subhedral to anhedral grains in the schists. It shows no particular textural association with graphite. Locally, it is overgrown and replaced by sphalerite. A late generation of pyrite is well

developed in graphite-bearing rocks where it may represent several volume per cent of the rock.

Graphite occurs in minor or trace amounts in biotite-amphibole schists throughout the area mapped. It is mainly present as fine to medium-sized, folded or kinked flakes aligned with the latest foliation and is often intergrown with concordant biotite (Plate 3-3-1) and, less commonly, with pyrite. Graphite occurs preferentially in garnet-free schists or at the contact between garnet-free schists and garnet-bearing schists or granodiorite (Figure 3-3-3). The association of chlorite with high concentrations of graphite in the crests of folds indicates that graphite formed during retrograde metamorphism. Also, some graphite precipitated during early retrograde metamorphism as indicated by the textural intergrowth of graphite and tremolite in clinopyroxene replacement textures (Plate 3-3-2).

A small amount of fine-grained, matte graphite is present along late shear zones cutting the regional foliation, and in narrow veins. This graphite formed during the last stages of retrograde metamorphism and stabilized at lower temperatures than the coarse flake graphite. The presence of pre-peak metamorphic graphite, early retrograde graphite and late retrograde graphite suggests that graphite precipitation took place during almost all stages of metamorphism.



Plate 3-3-1. Back-scattered electron micrograph of graphite-rich sample displaying close textural relationship between biotite (bt) and graphite (GP). Also shown is late, optically zoned pyrite (PY2) developed at the contact between graphite-rich and graphite-free layers. Width of field is 2.5 millimetres.



Plate 3-3-2. Natural light photomicrograph of sample G6/12-62 showing textural relationship between clinopyroxene, tremolite and graphite. See text for discussion. Width of field is 0.8 millimetres.

GRAPHITE-RICH ROCKS

Graphite-rich rocks are dark grey or rusty brown on weathered surfaces and locally characterized by a thin jarosite coating. Fresh surfaces are steel grey. The rocks are layered and have a lepidoblastic texture. Graphite occurs as flakes within the schists. Grades, expressed in terms of graphitic carbon content, are given in Table 3-3-2 (see also Figures 3-3-5 and 3-3-6). Individual layers may be graphite-rich or nearly barren. The graphite-rich rocks are soft and split along a foliation defined by the alignment of graphite flakes. Individual graphite flakes measure from 0.3 to 1.5 millimetres in diameter. The concentration of graphitic carbon reaches up to 24 weight per cent (Table 3-3-2 and Figures 3-3-5 and 3-3-6). The flakes have a metallic lustre, but locally are dull, indicating a lower degree of crystallinity.

Other major constituents, present in variable proportions, are quartz, feldspar, biotite and hornblende. Pyrite, either anhedral and optically zoned or cubic and unzoned, sphalerite and chalcopyrite comprise up to 5 per cent of the rock volume. The late-stage pyrite is the most abundant sulphide and occurs as optically zoned, medium to fine-grained patches in close textural association with graphite (Plate 3-3-3). Microprobe investigation of the optically zoned crystals reveals no variation in trace elements. The zoning is interpreted a result of to be variations in oxidation (de-sulphidation) of pyrite from core to rim. This zoned pyrite is intimately associated with sphalerite (Plates 3-3-4 and 3-3-3). Late pyrite also overgrows strongly resorbed pyrrhotite (Plate 3-3-3). It is also concentrated at the boundary between graphite-rich and graphite-free layers (Plate 3-3-1). These observations indicate that this pyrite and, by association, sphalerite, grew late with respect to graphite crystallization. Pyrrhotite has been identified in one sample as resorbed cores in late, optically zoned pyrite grains (Plate 3-3-3). Texturally, it appears to be associated with graphite flakes. Chalcopyrite is found in trace amounts, in rocks which also contain late pyrite and sphalerite. Sphalerite is present almost exclusively in graphite-bearing rocks as anhedral, undeformed grains. It is commonly associated with late pyrite. The base metal content of the graphite-rich samples is anomalous (Table 3-3-2), but not of economic interest. Sphalerite, chalcopyrite and zoned pyrite post-date graphite. Subhedral, bright pink to pale brown pleochroic titanite is a common mineral in graphitic rocks. Other minerals present in trace amounts are zircon and allanite. Biotite and sulphides are locally intergrown with graphite flakes. High-grade, coarse, crystalline graphite is found in the noses of outcrop-scale folds. Matte, finely crystalline graphite concentrations are also found in shear zones and late, post-ductile deformation veins (Plate 3-3-4).

PETROLOGIC INTERPRETATION

The presence of metamorphic clinopyroxene in hornblende-bearing rocks indicates minimum peak metamorphic temperatures were in excess of 750°C, consistent with granulite-grade metamorphism (Spear, 1981). In addition, garnet-biotite thermometry was used to constrain metamorphic conditions. Garnets from sillimanite-bearing

rocks exhibit a very gently decreasing Fe/Fe+Mg trend from core to rim that is consistent with increasing ambient temperature. It is interpreted to represent prograde zoning (Spear, 1991). The calculated peak metamorphic garnet-biotite temperature is $825 \pm 25^\circ\text{C}$ at a pressure of 750 ± 100 MPa (7.5 ± 1 Kbar) using the garnet-sillimanite-quartz-plagioclase barometer (Figure 3-3-7a), indicating conditions of granulite facies metamorphism.

Garnets from sillimanite-free, hornblende-bearing rocks display unzoned cores and increasing Fe/Fe+Mg trends at their rims. This is interpreted to be the result of diffusional re-equilibrium near the peak of metamorphism or during subsequent cooling (Spear, 1991). Calculated garnet-biotite temperatures for three sillimanite-free hornblende-bearing

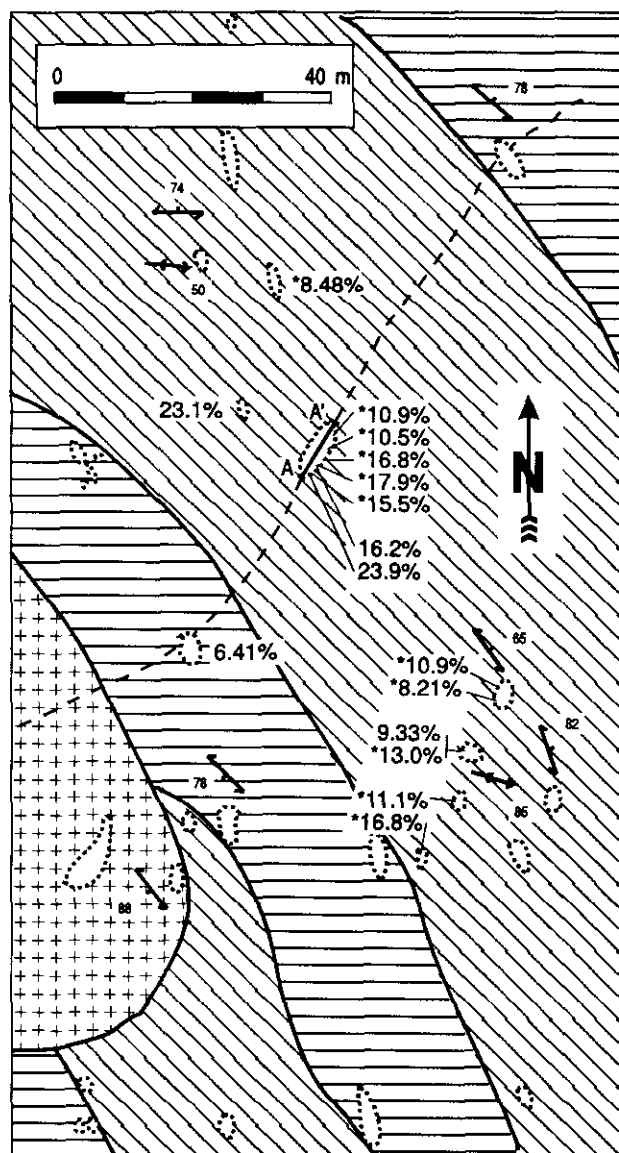


Figure 3-3-5. Detail of Figure 3-3-3 showing geology around the AA graphite deposit and graphitic-carbon contents from a number of trenches. A-A' is position of cross-section in Figure 3-3-6. * = data from Demczuk and Zbitnoff (1991).

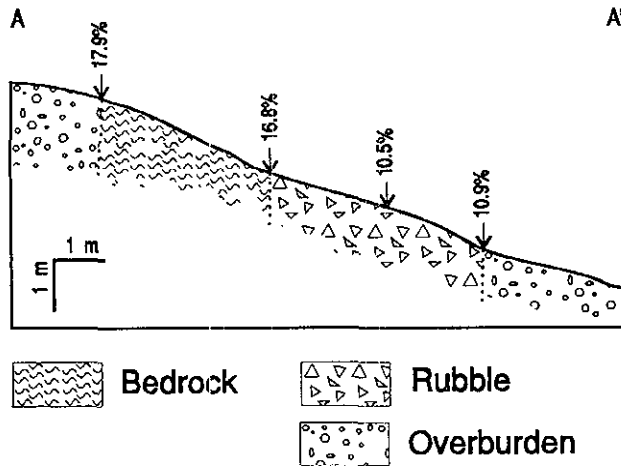


Figure 3-3-6. Cross-section through Trench 1 of the graphite deposit showing weight percentage of graphitic carbon. See Figure 3-3-5 for location.

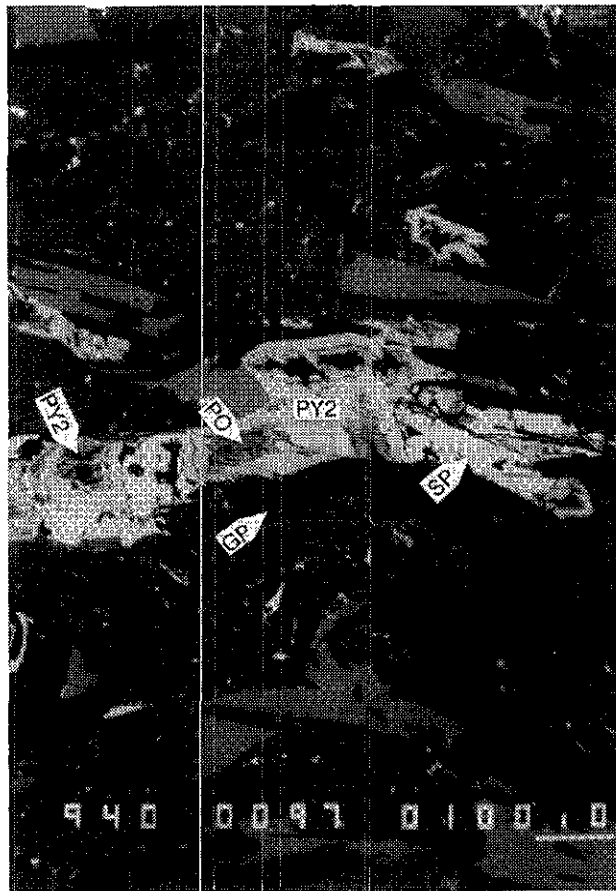


Plate 3-3-3. Back-scattered electron micrograph of late pyrite (PY2) cored by pyrrhotite (PO) and intergrown with sphalerite (SL). Note the close association of sulphides with graphite flakes (black). Scale bar is 100 microns.

rocks from different parts of the map area fall between 725° and 875°C, consistent with the presence of clinopyroxene and the sillimanite-schist calculated temperature (Figure 3-3-7b). Rare inclusions of graphite within these garnets suggest that some graphite persisted through metamorphic conditions well into the granulite field. Calculated retrograde (rim) temperatures for garnet-hornblende assemblages, Figure 3-3-7c, are consistently lower than garnet core - biotite temperatures. The stability field of titanite, as determined by Spear (1991), suggests that the graphite in equilibrium with titanite crystallized below 700°C, assuming a pressure of 500 MPa.

Replacement of clinopyroxene or cummingtonite by hornblende indicates that hornblende recrystallized extensively during the retrograde stages of metamorphism. Retrograde graphite is locally closely intergrown with tremolite (Plate 3-3-2), but such an association has not been found between graphite and hornblende. Clinopyroxene break-

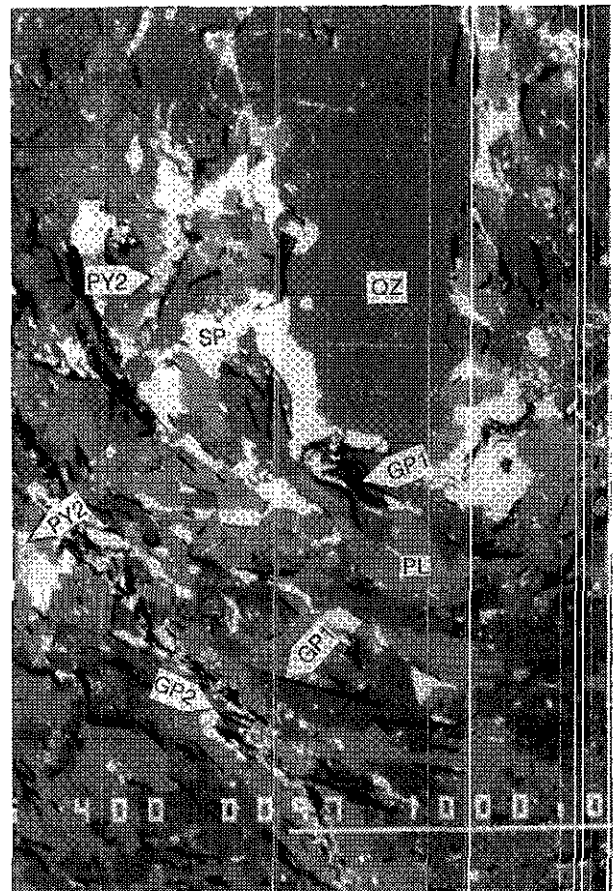


Plate 3-3-4. Back-scattered electron micrograph of graphite-bearing sample. (Brightness is proportional to density; GP1: pre to syntectonic graphite; GP2: post-tectonic vein graphite; SP: sphalerite; PY2: late pyrite; QZ: quartz; PL: plagioclase.) Quartz is concentrated in the core of a fold. Pre or syntectonic graphite coexists with post-tectonic graphite in a late vein. Coexistence of early and late pyrite is also shown (see text). Notice sphalerite concentration near graphite-free core part of fold. Scale bar is 1000 microns (1 mm).

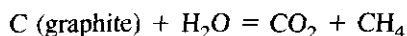
down to tremolite occurs between 500° and 600°C, assuming $X_{CO_2} = 0.25$ and 0.75 (Tracy and Frost, 1991). This provides an upper temperature limit for the formation of retrograde graphite consistent with that calculated from garnet-hornblende retrograde temperatures.

ORIGIN OF GRAPHITE MINERALIZATION

There are a number of possible sources of carbon from which the graphite may have originated:

- *in situ* reduction of organic matter during metamorphism;
- devolatilization of organic matter to produce CO_2 or CH_4 (or both) in the fluid phase;
- destabilization of early graphite to produce carbon-bearing volatiles (CO_2 and CH_4);
- decarbonation of carbonate minerals;
- injection of carbon-bearing fluids from the deep crust or mantle;
- a combination of the above.

In and around the deposit, low concentrations of prograde metamorphic graphite were probably derived by *in situ* graphitization of organic matter concentrated in discrete layers. Retrograde graphite involved migration of carbon dioxide and/or methane-bearing fluids prior to graphite precipitation. The fluids were derived from oxidation of pre-existing graphite or from the devolatilization of carbonate minerals. Calculations by Ohmoto and Kerrick (1977) indicate that the reaction:

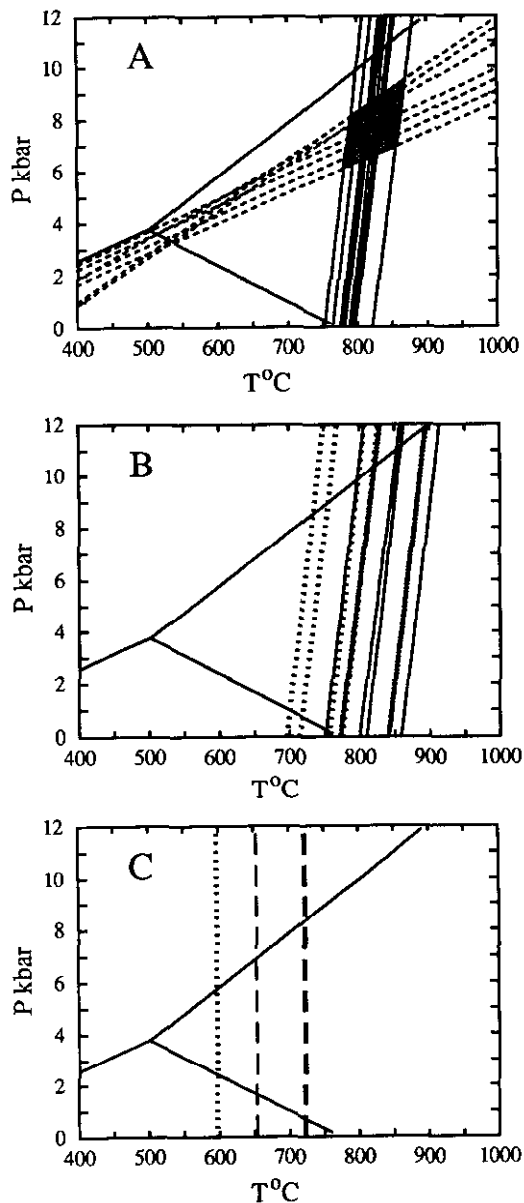


will proceed to the right with increasing temperature, favouring fluid enrichment in methane in a reducing environment and carbon dioxide in an oxidizing environment, at the expense of graphite. Hence, in a prograde metamorphic environment in which dehydration reactions take place, carbon will be concentrated in the fluid phase. Concentration of carbon in the fluid phase during prograde metamorphism followed by precipitation of graphite on cooling could account for remobilization and high graphite concentrations in permeable channels such as the crests of folds. Graphite could also have precipitated by the mixing of two fluids, one with a high X_{CO_2} and the other with either a high X_{H_2O} and/or X_{CH_4} . The hypothesis is based on a curved stability field of graphite in the C-O-H phase relation, as described by Rumble *et al.* (1982).

SUMMARY AND CONCLUSIONS

GENESIS OF GRAPHITE

The AA graphite deposit is hosted by metasedimentary biotite and biotite-hornblende schists intruded by granodioritic rocks. Medium to coarse-grained, premetamorphic graphite found as concentrations in discrete beds in the schists and as inclusions in prograde metamorphic minerals was subjected to temperatures in excess of 800°C at 750 MPa. This is well within the range of granulite facies metamorphism. Medium to coarse-grained, retrograde, syn-



Biotite - garnet (Ferry and Spear, 1978;
Hodges and Spear, 1982)

Hornblende - garnet (Graham and Powell, 1984)

Garnet - sillimanite - plagioclase - quartz
(Newton and Hazelton, 1981; Hodges and Spear,
1982; Ganguly and Saxena, 1984; Hodges and
Crowley, 1985)

Figure 3-3-7. (a) Calculated K_{eq} isopleths for iron-magnesium exchange between biotite and garnet and for the reaction: 2 anorthite = 2 grossular + sillimanite + 4 quartz, for sillimanite-bearing, hornblende-free biotite schist. (b) Calculated K_{eq} isopleths for iron-magnesium partitioning between biotite and garnet for three hornblende-bearing biotite-schists from the AA graphite deposit area. (c) Calculated K_{eq} isopleths for iron-magnesium partitioning between garnet and hornblende for three hornblende-bearing biotite-schists from the AA graphite deposit area.

tectonic graphite precipitated in the 500° to 700°C temperature range, as constrained by the textural associations between graphite and the minerals hornblende, tremolite and titanite. Concentration of syntectonic, early retrograde graphite at the crests of outcrop-scale folds indicates a structural control on graphite mineralization. Fine-grained graphite, post-dating ductile deformation, concentrated in shear zones and thin veins is the latest graphite generation observed in the area. It formed at low temperatures, consistent with the development of coexisting chlorite. This suggests that graphite mineralization took place through a wide range of temperatures during retrograde metamorphism.

EXPLORATION IMPLICATIONS

This study indicates that medium to high-grade crystalline flake graphite concentrations can be found within metasedimentary roof pendants of the Coast Plutonic Complex. Peak metamorphic conditions near the AA deposit reached granulite facies. The degree of crystallinity of natural graphite is directly related to the grade of metamorphism. High-grade graphite mineralization at the AA deposit is partly prograde metamorphic and partly retrograde metamorphic in origin. Because of the retrograde nature of some of the graphite and common intergrowths with micas, it is recommended that metallurgical studies be performed in the early stages of deposit evaluations. At the AA deposit, graphite-rich rocks occur along the crests of folds, a feature that is commonly observed in most of the eastern Canadian crystalline flake graphite deposits. Fold axes are vertical here, indicating that graphite-rich zones will be steeply plunging. Attention should be given to similar settings where fold axes plunge more gently to maximize efficient recovery by open-pit mining. Detailed investigation of graphite grade, continuity of graphite-bearing rocks, deposit size, shape and tonnage are beyond the scope of this work.

Granulite facies metamorphism is considered rare in the Coast Plutonic Complex. Only three other locations have been identified in a recent compilation by Read *et al.* (1991). This study may indicate that rocks of granulite facies could be more abundant than previously recognised. Prograde metamorphic graphite, if present in such metamorphic conditions, would have an excellent degree of crystallinity. In summary, there is excellent geological potential for economic crystalline flake graphite deposits within schists of the Coast Plutonic Complex.

ACKNOWLEDGMENTS

J.A. Roddick of the Geological Survey of Canada kindly provided preliminary information on the regional geology. J.M. Newell, B.C. Geological Survey Branch, and J.A. Roddick, Geological Survey of Canada, improved earlier versions of this manuscript.

REFERENCES

- Baer, A.J. (1973): Bella Coola - Laredo Sound Map-areas, British Columbia; *Geological Survey of Canada*, Memoir 372, 122 pages.
- Demczuk, L. and Zbitnoff, G.W. (1991): Geological and Geochemical Assessment Report on the AA 1-22 Claim Group; B.C. Ministry of Energy, Mines and Petroleum Resources, Assessment Report 21,649.
- Ferry, J.M. and Spear, F.S. (1978): Experimental Calibration of the Partitioning of Fe and Mg between Biotite and Garnet; *Contributions to Mineralogy and Petrology*, Volume 66, pages 113-117.
- Ganguly, J. and Saxena, S.K. (1984): Mixing Properties of Aluminosilicate Garnets: Constraints from Natural and Experimental Data, and Applications to Geothermobarometry; *American Mineralogist*, Volume 69, pages 88-97.
- Graham, C.M. and Powell, R. (1984): A Garnet-Hornblende Geothermometer: Calibration, Testing and Application to the Pelona Schist, Southern California; *Journal of Metamorphic Geology*, Volume 2, pages 13-21.
- Hand, G.P. (1992): Graphite; *Mining Engineering*, pages 560-561.
- Harries-Rees, K. (1992): Refractory Majors; *Industrial Minerals* Number 300, pages 23-43.
- Hodges, K.V. and Crowley, P.D. (1985): Error Estimation and Empirical Geothermobarometry for Pelitic Systems; *American Mineralogist*, Volume 70, pages 702-709.
- Hodges, K.V. and Spear, F.S. (1982): Geothermometry Geobarometry and the Al₂SiO₅ Triple Point at Mt. Moosilauke, New Hampshire; *American Mineralogist*, Volume 67, pages 1118-1134.
- Holroyd, W.G. and McCracken, W.H. (1992): Refractory Materials from China; *Industrial Minerals*, Number 293, pages 59-67.
- Kenan, W.M. (1992): Carbon and Changing Technologies; in Proceedings, Industrial Minerals '92, Toronto, *Blondon Information Services*, pages
- Newton, R.C. and Haselton, H.T. (1981): Thermodynamics of the Garnet-Plagioclase-Al₂SiO₅-Quartz Geobarometer; in Newton, R. C. *et al.*, Editors, Thermodynamics of Minerals and Melts, *Elsevier*, New York, pages 131-147.
- Ohmoto, H. and Kerrick, R. (1977): Devolatilization Equilibria in Graphitic Systems; *American Journal of Science*, Volume 277, pages 1013-1044.
- Read, P.B., Woodsworth, G.T., Greenwood, H., Grant, E.D. and Evenchick, C.A. (1991): Metamorphic Map of the Canadian Cordillera; *Geological Survey of Canada*, Map 1714A.
- Roddick, J. (in preparation): Rivers Inlet; *Geological Survey of Canada*, Open File Map.
- Rumble D., Ferry, J.M., Hoering, T.C. and Bouclet, A.J. (1982): Fluid Flow During Metamorphism at the Beaver Brook Fossil Locality, New Hampshire; *American Journal of Science*, Volume 282, pages 886-919.
- Simandl, G.J. (1992): Gîtes de Graphite de la Région de Gatineau; unpublished Ph.D. thesis, *École Polytechnique de Montréal*, 359 pages.
- Simandl, G.J., Jakobsen, D. and Fischl, P. (1992): Refractory Mineral Resources in British Columbia, Canada; *Industrial Minerals*, Number 296, pages 67-77.
- Spear, F.S. (1981): An Experimental Study of Hornblende Stability and Compositional Variability in Amphibolite; *American Journal of Science*, Volume 281, pages 697-714.
- Spear, F.S. (1991): On the Interpretation of Peak Metamorphic Temperatures in Light of Garnet Diffusion During Cooling; *Journal of Metamorphic Geology*, Volume 9, pages 379-388.
- Taylor, H.A., Jr. (1992): Graphite (Natural); in Mineral Commodity Summaries 1992, U.S. Department of Interior, Bureau of Mines, pages 76-77.
- Tracy, R.J. and Frost, B.R. (1991): Phase Equilibria and Thermobarometry of Calcareous, Ultramafic and Mafic rocks and Iron formations; in Contact Metamorphism, Kerrick, D.M., Editor, *Reviews in Mineralogy*, Volume 26, pages 207-290.

NOTES